1995A&A...295..171K

Astron. Astrophys. 295, 171–182 (1995)

ASTRONOMY AND ASTROPHYSICS

DR 1: a WO3 star in IC 1613 and its surrounding nebula, S3

Robin L. Kingsburgh[1] **and M.J. Barlow**[2]

[1] Instituto de Astronomía, Universidad Nacional Autónoma de México, P.O. Box 439027, San Diego, CA 92143-9027, USA
[2] Dept. of Physics & Astronomy, University College London, Gower St., London, WC1E 6BT, UK

Received 12 July 1994 / Accepted 25 August 1994

Abstract. We present an analysis of the WO3 star, DR 1, which is located in the dwarf irregular galaxy IC 1613, and is surrounded by an H II region which shows nebular He II 4686 Å in emission, a rare phenomenon in nebulae surrounding Wolf-Rayet stars. We have derived E(B–V) = 0.07 via a comparison of the observed Balmer line ratios to those predicted by theory, using the electron temperature of T_e = 17100 K derived from our nebular analysis. We find O/H = 4.99×10^{-5} by number for the nebula, in agreement with the O/H ratios found for other emission-line regions in IC 1613. We derive the following nebular mass fractions: X = 0.761, Y = 0.238 and Z = 0.00091. After allowance for the contribution by the nebular continuum, we have derived a stellar absolute magnitude of M_V = –3.6 for DR 1, a stellar effective temperature of T_* = 75000 K via a H I and He II Zanstra analysis, and a stellar luminosity of 10^6 $L_\odot$. A terminal wind velocity of v_∞ = 2850 km sec^{-1} is derived for DR 1 from the width of the strongest stellar emission lines. We also performed an abundance analysis of the stellar wind via a recombination theory analysis of the stellar emission-line features, and derive X(C) = 0.48, X(O) = 0.27 and X(He) = 0.25. These values are within the range found for other WO stars by Kingsburgh et al. (1994) and agree with those predicted by the Z = 0.004 massive star evolutionary models of Meynet et al. (1994), but not with their Z = 0.001 models. Our observations confirm the prediction that WO stars in low-metallicity galaxies should be much more luminous than their counterparts in higher metallicity galaxies.

Key words: stars: abundances – stars: Wolf-Rayet – galaxies: abundances – ISM: H II regions – galaxies: individual: IC 1613 – galaxies: ISM

1. Introduction

DR 1, located in the metal-poor dwarf irregular galaxy IC 1613, is surrounded by an H II region (No. 3 as listed by Sandage 1971; hereafter S3) with unusually strong nebular He II 4686 Å in emission. H II regions exhibiting He II emission are comparatively rare (Pakull 1991). D'Odorico & Rosa (1982) first noted that the star exciting S3 was a Wolf-Rayet star with particularly strong and wide 4686 Å and 5800 Å emission features. They classified it as WCpec or WC+WN, based on spectra covering the 4000–7000 Å range. We adopt the name DR 1 for this star, after the authors of the discovery paper. DR 1 and its surrounding nebula, S3, were subsequently studied by Davidson & Kinman (1982; hereafter DK82). Their spectra extended shortward to 3600 Å and they observed strong O VI 3811,34 Å emission from the star and suggested it may be a member of the WO class. The WO stars are a rare type of Wolf Rayet (WR) star, defined by Barlow & Hummer (1982) and Kingsburgh et al. (1994, hereafter KBS), whose spectra show strong lines of highly ionized stages of oxygen, carbon and doubly-ionized helium, thus distinguishing them from the WC and WN classes of WR star, whose spectra are dominated by lines of carbon and nitrogen respectively. The WO stars are presumably the most evolved of the WR stars, and their increased strength of oxygen lines is thought to reflect an increased oxygen abundance over the WC stars, whereby mass-loss stripping has revealed oxygen produced by α–particle capture by carbon nuclei. The WO stars could be immediate precursors to supernovae.

DK82 performed a Zanstra analysis on DR 1 using the nebular He II 4686 Å flux and derived a temperature of 110000 K for the WR star, adopting a blackbody distribution. However, a blackbody assumption probably does not well represent the far-UV/optical flux distribution of a WR star (Schmutz et al. 1989, 1992; Morris et al. 1993a) adding to the uncertainty in the derived $T_{\rm eff}$. DK82 derived low nebular helium and oxygen abundances, which should have been representative of those at the time of formation of the progenitor to the WR star. Other nebular analyses of S3 and additional H II regions in IC 1613 (e.g. Talent 1980; Peimbert et al. 1988) have also found IC 1613 to be extremely metal-poor.

Armandroff & Massey (1985) performed interference-filter imaging photometry on IC 1613 in search of Wolf-Rayet stars, and in their 'WC' filter, centered on 4649 Å, found DR 1 (their #6) to have a magnitude typical of WC stars. With subsequent

Send offprint requests to: R. Kingsburgh

© European Southern Observatory • Provided by the NASA Astrophysics Data System

1995A&A...295..171K

spectroscopy of DR 1 covering 4000–6000 Å, Armandroff & Massey (1991) classified it as WC4-5.

Garnett et al. (1991) have also observed DR 1, and suggested that the star may be a WO4 star, based on existing spectra. They also performed a stellar-temperature analysis, using the ratio of the ionizing photon fluxes in the H^0 and He^{2+} continua implied by the nebular Hβ and He II 4686 Å fluxes in comparison with the ratios predicted by the plane-parallel hydrogen/helium non-LTE stellar atmosphere models of Husfield et al. (1984) and Clegg & Middlemass (1987). With these assumptions, T_{eff} was found to range between 75000 K for the log g = 4.5 models, and 90000 K for the log g = 5.5 models.

We have obtained new WHT observations of DR 1 and its surrounding nebula, where our spectral coverage extends from 3200–8600 Å, and present a comprehensive analysis of both the central star and nebula. Equivalent widths of the strongest emission line features for DR 1 have been presented by KBS, where we classified the star as WO3, from the relative stellar emission line equivalent widths after subtraction of the nebular continuum contribution. If this subtraction is not done, not only are the stellar emission line equivalent widths underestimated, but the continuum level for the blue O VI 3811,34 Å feature is overestimated compared to the red classification lines, and an incorrect later spectral type derived.

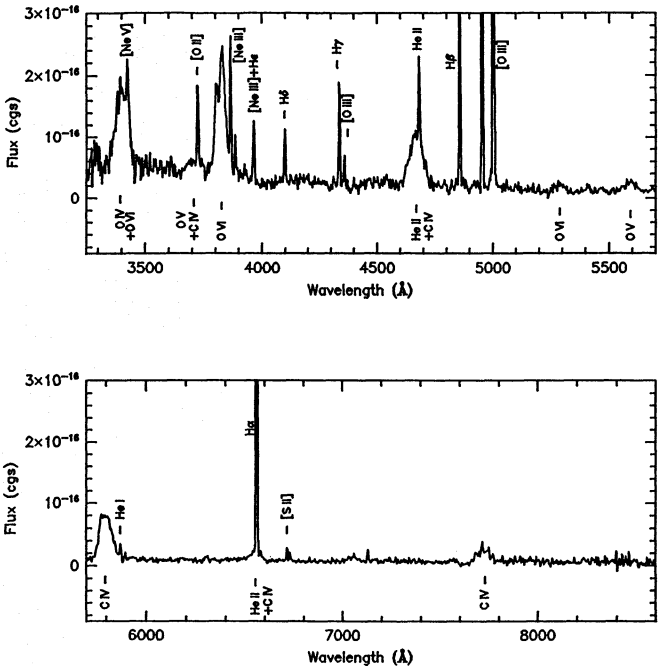

Fig. 1. Observed F_λ (ergs cm^{-1} sec^{-1} $Å^{-1}$) vs λ (Å) distribution for narrow slit, central 4.8 arcsec extraction of DR 1. The strongest stellar features are labelled below the spectrum, and nebular features are labelled above

2. Observations and data analysis

Service observations of DR 1 and its surrounding H II region, S3, were obtained with the 4.2-m William Herschel Telescope at La Palma, in January 1992. The ISIS spectrograph was used at the f/11 Cassegrain focus, with two EEV CCDs as detectors, one for each arm of the spectrograph. Each chip had 1280 pixels along the dispersion direction and was binned to yield 400 pixels along the spatial direction. The slit length was 4 arcmin, yielding a plate scale of 0.6 arcsec per pixel. The slit position angle was 55° east of north. A dichroic was employed to split the light beam; the blue spectral coverage was from 3000–6200 Å and the red spectral coverage was from 5300–8900 Å. The B158R and R158R gratings were used, blazed at 3600 Å and 6500 Å respectively, yielding dispersions of 120 and 121 Å mm^{-1}. Two 1500 second narrow-slit exposures were obtained using a 1 arcsecond wide slit, and one 900 second wide-slit exposure was obtained with a 6.75 arcsecond slit. A wide-slit observation of Feige 24 (Oke 1990) was also obtained, for flux calibration purposes.

The spectra were reduced using IRAF[1]. The bias frames were averaged and subtracted from all spectral images. The images were then divided by a normalized flat field. The cosmic rays were cleaned interactively. The wavelength calibration was performed using a 5th order fit to 41 Cu-Ar arc lines for the red spectra, and a 4th order fit to 47 arc lines for the blue spectra. The derived dispersions were 2.77 Å/ $pixel^{-1}$ in the red and 2.70 Å/ $pixel^{-1}$ in the blue. Background subtraction was performed, and three extractions were made for both the wide and narrow slit spectral images: one of only the central star (4.8 arcsec in width), one of the area with the brightest nebular emission (18 arcsec), and one containing all the nebular emission (90 arcsec). After correcting for atmospheric extinction using the mean La Palma extinction coefficients, the spectra were flux calibrated. The red and blue spectra were then joined; the region of overlap for both nebular and standard star spectra neatly joined in terms of both slope and flux level. As the red spectra had significantly higher S/N in the overlapping region, they were adopted with full weight.

The spectral analysis was performed using DIPSO (Howarth & Murray 1990) at the UCL STARLINK node. The fluxes of all nebular lines were measured, from both nebular extractions. To obtain high S/N on the faint nebular lines, we used fluxes from the extraction over the central 18 arcsec, and adopted fluxes from the full 90 arcsec extraction for the strongest lines only. To measure the fluxes for nebular lines which were situated on top of broad stellar lines, a gaussian (or polynomial) fit was first made to the central star feature (or side of central star feature), which was then subtracted from the spectrum and the nebular fluxes measured. Stellar emission line fluxes and equivalent widths were initially measured for DR 1 from the central extraction, however the central star spectra were later corrected for the presence of the nebular continuum, and the fluxes and equivalent widths re-measured (see Sect. 4).

Figure 1 presents the nebular spectrum of S3, with both nebular and central star features marked.

[1] IRAF is distributed by National Optical Astronomy Observatories, which is operated by the Association of Universities for Research in Astronomy, Inc., under contract to the National Science Foundation

© European Southern Observatory • Provided by the NASA Astrophysics Data System

1995A&A...295..171K

3. Nebular analysis

3.1. Reddening

Table 1 presents the nebular line fluxes (F_λ), extracted as described in the previous section, on a scale where F(Hβ) = 100. (Hereafter, all line fluxes given in the text will be expressed with this scale.) Dereddened fluxes (I_λ) are also presented in Table 1, along with the galactic reddening function f(x) of Seaton (1979). We have adopted c(Hβ)=0.1 (or E(B–V)=0.069), which yields dereddened I(Hα):I(Hβ):I(Hγ):I(Hδ) ratios of 276:100:47.3:25.6, which compare well to the thoretical ratios of 277:100:47.4:26.3 (Hummer & Storey 1987) for an electron temperature of 17000 K (Sect. 3.2)[2]. Additional evidence for adopting a low value of reddening towards DR 1 comes from the Galactic foreground reddening map of Burstein & Heiles (1982) which yields E(B–V)<0.03 for the direction towards DR 1, and the H I column density map for IC 1613 of Lake & Skillman (1988) which yields E(B–V)<0.01 for this location, if the Fitzpatrick (1985) N(H I)/E(B–V) ratio for the SMC is used. DK82 derived E(B–V) = 0.08 for S3, from their observed Hα/Hβ ratio. Garnett et al. (1991) derived E(B–V) = 0.03±0.10 from their Hβ/Hγ/Hδ ratios.

Agreement between our observed line fluxes and those of DK82 is generally better than 5%. The only flux which differs significantly is He I 4471 Å, where we measure 4: and DK82 measure 1.6. As our He I 4471 Å flux is somewhat uncertain, we have derived the He^+/H^+ abundance from the λ5876 Å feature only (Sect. 3.3).

Table 1. Observed (F) and dereddened (I) nebular line fluxes for c(Hβ) = 0.1

λ(Å)	ID	f(x)	F/F(Hβ=100)	I/I(Hβ=100)
3426	[Ne V]	0.334	7::	7.5::
3727	[O II]	0.256	55.8	59.2
3868	[Ne III]	0.230	50.3	53.0
3888	H8, He I	0.227	18.4	19.4
3968	[Ne III]+Hϵ	0.210	30.0	31.5
4101	Hδ	0.182	24.5	25.6
4340	Hγ	0.127	45.9	47.3
4363	[O III]	0.121	13.5	13.9
4471	He I	0.095	4:	4:
4686	He II	0.043	22.9	23.1
4711	[Ar IV]	0.037	4.5:	4.5:
4740	[Ar IV]	0.030	5.58	5.62
4861	Hβ	0.000	100	100
4959	[O III]	-0.024	189	188
5876	He I	-0.215	7.5	7.1
6563	Hα	-0.320	297	276
6583	[N II]	-0.323	6.9:	6.4:
6678	He I	-0.336	1.4:	1.3:
6717	[S II]	-0.342	9.46	8.73
6731	[S II]	-0.344	6.25	5.78
7065	He I	-0.387	3.2:	2.9:
7135	[Ar III]	-0.396	7.03	6.42
7325	[O II]	-0.419	3.2:	2.9:
7753	[Ar III]	-0.467	5:	4.5:

3.2. Temperature and density diagnostics

The electron temperature T_e derived from the [O III] 4959/4363 Å ratio of 13.66±0.67 was 17100±500 K, while the [S II] 6717/6731 Å ratio was 1.51±0.057, consistent with the low density limit, hence an electron density of 100 cm^{-3} was adopted for the abundance analysis. The error on T_e is based on the 5% measurement error estimated for the 4363 Å flux, and the error on the [S II] ratio is based on the 3% measurement errors estimated for the fluxes of 6717,31 Å. The [Ar IV] 4711/4740 Å ratio was 0.81:, which yields n_e(Ar IV) = 7000 cm^{-3}; this value is uncertain as the [Ar IV] line fluxes are uncertain, due to their lying on the stellar λ4686 feature. The ratio is approaching its low density limit.

The electron temperature derived here agrees within the errors with that of DK82 who found T_e(O III) = 16300±1000 K. The high electron temperature is consistent with the extremely low metallicity found for IC 1613 (Sect. 3.3).

3.3. Nebular abundance analysis

Abundances were derived from the collisionally excited lines by solving the equations of statistical equilibrium using the program EQUIB (written by S. Adams and I. Howarth). T_e = 17100 K and n_e = 100 cm^{-3} were adopted for all ions. He^+/H^+ ratios were derived allowing for collisional corrections following Clegg (1987). Hydrogen and He II recombination coefficients were taken from Hummer & Storey (1987). Table 2 presents the ionic abundances for He^+, He^{2+}, N^+, O^+, O^{2+}, Ne^{2+}, Ar^{2+}, Ar^{3+} and S^+ relative to H^+. We used the ionization correction factors derived by Walton et al. (1994) from detailed photoionization models, which are also listed by Kingsburgh & Barlow (1994). Total elemental abundance ratios are also presented in the final column of Table 2. See Table 5 of Kingsburgh & Barlow (1994) for references for the atomic data used for this nebular analysis.

Following the abundance analysis, the theoretical nebular recombination continuum was calculated, using the routine NEBCONT in DIPSO, written by Dr. J. P. Harrington. This program determines the H and He b–f and f–f continua, as well as the H I and He II 2-photon continua, normalized to a given I(Hβ) and relative helium line fluxes. As the metallicity of IC 1613 is so low, heavier elements give an insignificant contribution to the nebular continuum. A NEBCONT was calculated for both narrow- and wide-slit extractions. Figure 2 plots our wide slit spectrum, with the calculated nebular continuum shown as the dashed line below.

[2] Note that the contribution from the stellar He II+C IV 6560 Å feature has been subtracted from the total Hα flux.

© European Southern Observatory • Provided by the NASA Astrophysics Data System

1995A&A...295..171K

Table 2. Nebular abundances by number

element	ion	λ(Å)	n_{ion}/n_{H^+}	ICF	n_X/n_H
He	He^+	5876	0.0572		
	He^{2+}	4686	0.0207	–	0.078
N	N^+	6583	3.79×10^{-7}	14.5	5.51×10^{-6}
O	O^+	3727	3.42×10^{-6}		
	O^{2+}	4959	3.71×10^{-5}	1.2	4.99×10^{-5}
Ne	Ne^{2+}	3868	9.15×10^{-6}	1.3	1.23×10^{-5}
Ar	Ar^{2+}	7135	1.92×10^{-7}		
	Ar^{3+}	4740	3.00×10^{-7}	1.1	5.28×10^{-7}
S	S^+	6725	1.13×10^{-7}	14.6	1.65×10^{-6}

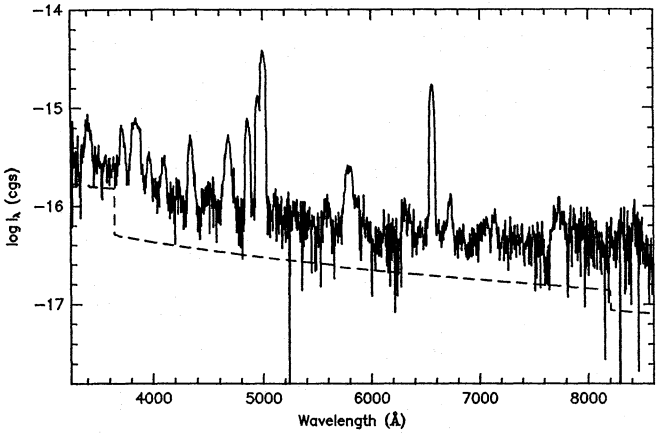

Fig. 2. I_λ vs λ for the wide-slit, central 4.8 arcsec extraction of DR 1, in logarithmic cgs flux units, dereddened using E(B–V) = 0.07. The dashed line below the spectrum is the nebular continuum calculated for the observed log F(Hβ) = –13.64

3.4. Discussion of nebular abundances

Table 3 presents the nebular abundances for S3 expressed on a logarithmic scale where H = 12.0, together with abundances for the supernova remnant S8, in IC 1613, listed by Peimbert et al. (1988), who derived abundances for the SNR via the models of Dopita et al. (1984) and found the abundances to be representative of the swept up ISM of IC 1613, rather than the ejecta of the supernova. Abundances for galactic, SMC and LMC H II regions (Dufour 1984) are also presented for comparison in Table 3. From our abundances, we derive the following mass fractions for S3: X = 0.761, Y = 0.238 and Z = 0.00091.

3.4.1. Helium

Our helium abundance of 0.078 (by number) compares well with that of DK82, who derived He/H = 0.073±.009. A similar He/H ratio, 0.075, was found for S8 by Peimbert et al. (1988).

3.4.2. Oxygen

The derived oxygen abundance in the present study, O/H = 4.99×10^{-5} by number, is in reasonable agreement with that of DK82 who derived O/H = 7.5×10^{-5}; our O/H is slightly lower as we have adopted a higher T_e. We also have reasonable agreement with the O/H ratio found for S8 by Peimbert et al. (1988), O/H = 6.76×10^{-5}. Also, Peimbert et al. re-derived the oxygen abundance for the A17 region (Hodge 1978), which encompasses the S10 and S13 regions of Sandage (1971), using the line intensities of Hunter & Gallagher (1985) and models of Stasinska (1980, 1982). They found O/H values ranging from 5×10^{-5} to 6.3×10^{-5}. We find no evidence for oxygen depletion in S3 relative to the other H II regions in IC 1613, whereas oxygen depletion is seen in some galactic WR nebulae (Esteban et al. 1992). Indeed, the relative uniformity of oxygen abundances within IC 1613 indicates that little mixing of the ISM has occurred, a common feature of dwarf irregular galaxies (Skillman et al. 1989).

3.4.3. Nitrogen

The N/H ratio which we have derived, 5.51×10^{-6} by number, is only 14% higher than that found for S8 by Peimbert et al. The N/O ratio of 0.11 is somewhat high, compared to S8 and galactic and Magellanic Cloud H II regions (see Table 3) or the N/O ratio of 0.03 found by Garnett (1990) for dwarf irregular galaxies. Our enhanced nitrogen abundance derived from the [N II] 6584 Å line may be uncertain however, due to the combination of a weak λ6584 flux (although the value is in good agreement with DK82) and a high ionization correction factor (Table 2). Hubble Space Telescope observations in the UV would be required to verify that the higher stages of ionization of nitrogen are indeed present, and to derive a more accurate overall abundance. If the high N/H ratio is real, this could indicate that the nebula surrounding DR 1 is contaminated by ejecta material, as seen in some galactic WR nebulae (e.g. Kwitter 1984; Esteban et al. 1992) and in one LMC WR nebula (Garnett et al. 1993). Although these other nebulae also show typically a factor of two increase in their He/H ratio over the local ISM value (e.g. see Table 2 of Chu 1991), which is not found for DR 1, this may be because S3 around DR 1 is a much larger and more massive nebula compared with those studied by Esteban et al. (1992), and any enrichment effects have been diluted, thus most the abundances in S3 reflect those of the ISM in IC 1613.

3.4.4. Neon

From our analysis, we have found a relatively high Ne/O ratio of 0.25 for S3, compared to 0.16 found for H II regions in the Galaxy, LMC and SMC (Dufour 1984, see Table 3). A similarly high Ne/O ratio of 0.30 was found for S8 by Peimbert et al. (1988), which would seem to imply that the Ne/O ratio in IC 1613 really is high, compared to found for the SMC, LMC and Milky Way. Neon and oxygen are both believed to trace the metallicity of the original star-forming regions (Henry 1990). It

© European Southern Observatory • Provided by the NASA Astrophysics Data System

1995A&A...295..171K

is unlikely that the observed Ne/O enhancement is due to processed material from the WO star's wind, as neon is produced from He-burnt material, whereas the enrichment seen in other WR nebulae (including the nebula G2.4+1.4 around the galactic WO1 star Sand 4) comes from the products of the CNO cycle (Esteban et al. 1992).

If the [Ne V] 3426 Å line is used to derive the Ne^{4+} abundance, then for an electron temperature of 17100K, a Ne^{4+}/H^+ ratio of 1.12×10^{-7} is derived. Allowing for the Ne^{2+} abundance derived in Table 2 and adopting an ICF of 1.5 to account for the presence of Ne^{3+}, a final ratio of Ne/H = 1.39×10^{-5} is derived, only 13% higher than derived in Table 2. The [Ne V] line is badly blended with the stellar O IV feature at 3400 Å, and its flux is accordingly very uncertain. However, even a factor of two decrease in its flux would not alter the final neon abundance significantly.

Similarly, Esteban et al. (1992) derived somewhat high Ne/O ratios for the WR nebula G 2.4+1.4 surrounding Sand 4. They list Ne/O = 0.20:, 0.26, 0.29 and 0.43 for four areas in the nebula, where the spread is likely due to observational error rather than real variations across the nebulae. Additionally, Esteban et al. (1992) derived average Ne/O ratios of 0.23 and 0.25 for the WR nebulae NGC 3199 and S 308 respectively, which both surround WN5 stars. The probable reason for the difference between the Ne/O values found by us and by Esteban et al. (1992) vs. those given by Dufour (1984) is a different approach to deriving the ionization correction factors (ICF). We (and Esteban et al.) have adopted the 'standard' ICF for Ne: O/O^{2+}, whereas Dufour (1984) adopted an ICF based on photoionization models, which ultimately gave lower Ne/H ratios by comparison. As the Ne/H ratio derived by us for DR 1 using the 'standard' ICF and Ne^{2+}/H^+ ratio is essentially equal to the Ne/H ratio derived using the Ne^{2+}/H^+ plus Ne^{4+}/H^+ ratios, we adopt the neon abundance in Table 2 as it stands.

3.4.5. Argon, sulphur

The argon abundance derived here agrees well with that of DK82. The sulphur abundance has not been previously derived for S3, and agrees with the sulphur abundance found for S8 by Peimbert et al. (1988).

4. Stellar analysis

The stellar emission-line equivalent widths for DR 1 were measured from the narrow-slit spectrum, after subtraction of the nebular continuum (Sect. 3.3). These equivalent widths (EW) are presented in Table 4. Quantities flagged with a single colon are uncertain to within 30% and fluxes flagged with a double colon are uncertain to within 50%. The equivalent widths were then converted into absolute line fluxes by multiplying them by F_λ, the continuum flux at the wavelength λ of the line, as measured on the nebular continuum-subtracted wide-slit spectrum. As E(B–V) = 0.069 was derived from the nebular analysis, it was also adopted for the stellar analysis. The observed and dereddened stellar line intensities are presented in Table 4. Identifications for the transitions, and their estimated fractional contribution to each stellar emission feature, are also given in Table 4. The derivation of a particular ion's fractional contribution to a blended feature was estimated by using the strengths relative to unblended lines predicted by recombination theory (as discussed in Sect. 8.3 of KBS) and subtracting these from the blend; the remaining line flux is due to the other contributor(s).

DR 1 was classified as a WO3 star by KBS, using the equivalent widths listed in Table 4 of this paper and the line classification ratios listed in Table 8 of KBS. The subtypes for the WO stars range from WO5 (lowest excitation) to WO1 (highest excitation), and follow on immediately from the WC4 subtype of the WC class. DR 1 is the first member of the WO3 class. Only five other WO stars are known: Sand 1 and Sand 2 are WO4 systems in the SMC and LMC respectively, Sand 4 is a galactic WO1 star, Sand 2 is a galactic WO2 star, and MS 4 is a galactic WO5 system.

In order to derive magnitudes for DR 1, we used the nebular continuum-subtracted wide-slit spectrum, and measured the stellar continuum flux at 5480 Å, which was found to be 2.0×10^{-17} ergs cm^{-2} s^{-1} $Å^{-1}$, corresponding to V = 20.7 for this WO3 star. DK82 estimated V~20.1 for DR 1, but from the in-aperture Hβ flux which they quote, we estimate that the nebular continuum contributed about half of the continuum flux level that they measured, bringing the stellar flux into closer agreement with that measured here.

Saha et al. (1992) derived a distance modulus m–M = 24.1 for IC 1613 from a study of its RR Lyrae population. Combining this with our measured V = 20.7, and A_V = 0.2 (for R = 3.1), M_V = –3.6 is obtained for this WO3 star, 1.1 magnitudes brighter than derived by KBS for the WO4 star Sand 2 in the LMC and 1.8 magnitudes brighter than KBS derived for the WO2 star Sand 5 in the galactic open cluster Be 87. Smith & Maeder (1990) discussed how the evolutionary models of Maeder (1990) predict that at lower Z, stars with a given (C+O)/He ratio will be of higher luminosity than stars of similar subtype located in regions of higher Z, in accord with what is found here (see Sect. 4.1).

A wind terminal velocity of v_∞ = 2850 km sec^{-1} is derived from the FWZI/2 of the C IV 5801,12 Å feature, after correction for the doublet separation. In KBS, we showed that the FWZI/2 of the C IV 5801,12 Å feature was representative of the terminal wind velocity, via a comparison of the terminal velocity given by the black absorption edge of the C IV 1550 Å feature with expansion velocities derived from the FWHM and FWZI/2 of various WO optical emission lines. The C IV+He II 4658+86 feature of DR 1 yielded a FWZI/2 expansion velocity of 2750 km/sec. Comparing with the wind terminal velocities derived for other WO star by KBS, DR 1 has the lowest terminal velocity amongst the WO stars. The next lowest terminal velocity is the 4200 km sec^{-1} derived for the WO4 component of Sand 1 by KBS, a star located in the SMC, the next lowest metallicity galaxy in the sample.

Other narrow-lined early-WC type stars have been found in the central regions of M33 (Schild et al. 1990) and of NGC 300 (Schild & Testor 1991), where both central regions are of

© European Southern Observatory • Provided by the NASA Astrophysics Data System

1995A&A...295..171K

Table 3. Logarithmic[a] nebular abundances

	He/H	O	N	Ne	Ar	S	N/O	Ne/O
S3[b]	0.078	7.70	6.74	7.09	5.72	6.82	0.11	0.25
S8[c]	0.075	7.83	6.68	7.31	–	6.30	0.07	0.30
Gal H II[d]	0.100	8.70	7.57	7.90	6.42	7.06	0.074	0.16
LMC H II[d]	0.082	8.43	6.97	7.64	7.64	6.85	0.035	0.16
SMC H II[d]	0.081	8.02	6.46	7.22	5.78	6.49	0.028	0.16

Notes to Table 3: [a] He/H, N/O and Ne/O ratios are by number. Other abundances are logarithmic relative to H, where H = 12.0. [b] S3 abundances from this paper. [c] S8 abundances from Peimbert et al. (1988). [d] Galactic, LMC and SMC H II region abundances from Dufour (1984).

Table 4. Emission line equivalent widths and fluxes for DR 1

λ (Å)	ID	EW (Å)	F (ergs cm^{-2} sec^{-1})	frac	I (ergs cm^{-2} sec^{-1})	$I_{component}$ (ergs cm^{-2} sec^{-1})
3400,34	O IV (3d ^{2}D–3p ^{2}P^0)	204±5	2.12×10^{-14}	0.86	2.89×10^{-14}	2.49×10^{-14}
	O VI (7–6,11–8)			0.14		(3.94×10^{-15})
3690	O V (3d′ ^{3}D^0–3p′ ^{3}D)	70:	5.62×10^{-15}:	0.78	7.52×10^{-15}:	5.90×10^{-15}
	C IV (9–6,15–7,14–7)			0.22		(1.61×10^{-15})
3811,34	O VI (3p ^{2}P^0–3s ^{2}S)	360±30	2.48×10^{-14}		3.30×10^{-14}	
4658,86	C IV (6–5,8–6)	330±20	1.48×10^{-14}	0.70	1.88×10^{-14}	1.31×10^{-14}
	He II (4–3)			0.30		5.77×10^{-15}
5290	O VI (8–7)	55	1.26×10^{-15}		1.55×10^{-15}	
5411	He II (7–4)	30::	5.5×10^{-16}::	0.69	6.7×10^{-16}::	4.6×10^{-16}
	C IV (14–8)			0.31		2.1×10^{-16}
5470	C IV (10–7)	20::	4.2×10^{-16}::		5.1×10^{-16}::	
5590	O V (3d ^{3}D–3p ^{3}P^0)	120	2.46×10^{-15}		2.98×10^{-15}	
5801,12	C IV (3p ^{2}P^0–3s ^{2}S)	690±40	1.41×10^{-14}		1.69×10^{-14}	
6561	He II (6–4)	110::	1.8×10^{-15}::	0.8	2.1×10^{-15}::	1.7×10^{-15}
	C IV (12–8)			0.2		4.0×10^{-16}
7062	C IV (9–7)	75:	1.10×10^{-15}		1.27×10^{-15}	
7726,36	C IV (7–6,11–8,14–9)	260:	3.77×10^{-15}		4.27×10^{-15}	

approximately solar metallicity. Schild et el. (1990) found a dependence of expansion velocities on galactocentric distance for a sample of WC4-5 stars in M33, whereby the FWHM of the C IV 5801,12 Å features of stars located towards the centre of M33 was smaller than for stars with larger galactocentric distances; the expansion velocities were correlated with metallicity in the sense that smaller expansion velocities were found in higher metallicity regions. This trend was further substantiated by Willis et al. (1992) with an extended sample of WC4-5 stars in M33. Armandroff & Massey (1991) also confirmed the trend seen in M33, and found a similar trend for galactic WC stars. The trend for WO stars seems to be the opposite of this, however. The WO stars in the lowest metallicity galaxies, IC 1613 and the SMC, have the lowest wind expansion velocities, while the galactic WO2 star Sand 5 has the highest wind expansion velocity. General evolutionary models will need take these effects into account.

A summary of the stellar parameters derived above for DR 1 is presented in Table 5, as well as its temperature (T_*), luminosity (log L), radius (R_*) and mass loss rate ($\dot{M}$) derived below.

4.1. Zanstra temperature analysis

We have performed a Zanstra temperature analysis of DR 1 using the dereddened stellar flux in the visible and the integrated nebular Hβ and He II 4686 Å fluxes to estimate the ratio of the optical stellar flux to the photon fluxes shortward of the ionization edges of H^0 and He$^+$ at 912 Å and 228 Å respectively. Following the formalism of Clegg & Middlemass (1987), we derived the Zanstra ratios, R_{ion},

$$R_{ion} = \frac{n_{ion}}{F_\lambda(\lambda^*)} \quad (1)$$

where n_{ion} is the number of emergent photons at the stellar surface in the photoionization continua of H or He$^+$ (cm^{-2} s^{-1})

© European Southern Observatory • Provided by the NASA Astrophysics Data System

1995A&A...295..171K

Table 5. Summary of properties of DR 1

Spectral Type:	WO3
V	20.7
E(B–V)	0.069
m–M	24.1[a]
M_V	–3.6
v_∞	2850 km sec^{-1}
T_*	75000±8000 K
B.C.	–6.6
log(L/L$_\odot$)	6.0±0.2
R$_*$/R$_\odot$	6±1
$\dot{M}$	2.9×10^{-5} M$_\odot$ yr^{-1}

[a] Saha et al. 1992

and F_λ is the stellar continuum flux per unit wavelength emergent at the stellar surface (in erg cm^{-2} s^{-1} Å^{-1}), measured at wavelength λ^*. Using standard recombination theory, equation (1) may be expressed explicitly as

$$R(He\ II) = \frac{1.03\times10^{12}\ t^{0.29}\ I(4686)}{F_{star}(\lambda^*)} \quad (2)$$

$$R(H\ I) = \frac{2.08\times10^{12}\ t^{0.06}\ I(4861)}{F_{star}(\lambda^*)} \quad (3)$$

where t is the nebular electron temperature in units of 10^4 K and I is the dereddened nebular line flux at Earth, in cgs units. $F_{star}(\lambda^*)$ is the observed stellar flux at Earth and has been evaluated at 4200 Å, 4400 Å and 4800 Å. These wavelengths were chosen to avoid areas in the spectrum where stellar features are present (which add to the uncertainty in estimating the continuum height), and to minimize the wavelength separation between recombination lines and continuum so that reddening uncertainties would have a minimal effect. The Wolf-Rayet model atmospheres used to calculate the optical to far-UV stellar flux ratios were the $\beta = 1$ pure helium extended models of Schmutz et al. (1989) and the $\beta = 2$ pure helium models of Schmutz et al. (1992). The effects of the neglect of carbon and oxygen opacity have been discussed by Schmutz et al. (1992). They conclude that although such opacity could significantly affect the emergent flux distribution, the assumption of an extended $\beta = 1$ or $\beta = 2$ atmospheric structure gives the most important effects.

As the distance to DR 1 is known (660 kpc, see above), the total ionizing photon rates from the star in the H^0 and He^+ continua, N(H I) and N(He II), can be derived, where N_{ion}, in units of s^{-1}, is equal to n_{ion} (given by the numerator of equations 2 and 3) multiplied by $4\pi D^2$.

In order to derive the total Hβ flux for S3, we adopted the total Hα flux from the CCD survey of H II regions in IC 1613 of Hodge et al. (1990), who measured F(Hα) = 8.03×10^{-13} ergs cm^{-2} s^{-1} for S3. We dereddened this flux using E(B–V) = 0.069 and estimate a total I(Hβ) of 3.40×10^{-13} ergs cm^{-2} s^{-1} for S3 using our dereddened I(Hα)/I(Hβ) ratio from Table 1. The dereddened integrated Hβ flux measured in our wide-slit spectrum is 9.81×10^{-14} ergs cm^{-2} s^{-1}, and as expected, underestimates the total nebular flux, since the slit width was only 6.75 arcsec, compared with the Hα nebular diameter of 70 arcsec that we estimate from our long-slit spectrum. Price et al. (1990) have also measured an integrated F(Hα) for S3, with the ratio of the integrated Hα fluxes measured for S3 by the Hodge and Price surveys respectively being 2.78. As the survey of Hodge et al. (1990) extended to a fainter surface brightness level (2×10^{-17} ergs cm^{-2} s^{-1}arcsec^{-2}), we adopted the Hodge et al. flux.

The nebular He II emission was found to extend ±5 arcsec from the WO3 star in our narrow long-slit spectra, consistent with the estimate of ±6 arcsec of Garnett et al. (1991). The observed drop in the nebular He II surface brightness with distance from DR 1 implied that our 6.75 arcsec-wide long-slit spectrum should have encompassed almost all the nebular He II emission. With the assumption of azimuthal circular symmetry about DR 1, the surface brightness distribution along the narrow long-slit spectra implied an integrated nebular He II λ4686 flux of 1.22×10^{-14} ergs cm^{-2} s^{-1}; while simply multiplying the total nebular λ4686 flux measured in the narrow long-slit spectrum by 6.75 (the ratio of the widths of the wide and narrow slits) yielded 1.21×10^{-14} ergs cm^{-2} s^{-1}. Finally, in order to derive the total nebular He II 4686 Å flux in the 6.75 arcsec-wide long-slit spectrum, we measured the integrated stellar and nebular λ4686 flux in the spectrum (as the spectral resolution was degraded in the wide-slit spectrum, making it impossible to deconvolve the stellar and nebular components) and subtracted the stellar flux contribution given in Table 4 from the total to give a nebular flux of F(4686) = 1.28×10^{-14} ergs cm^{-2} s^{-1}. We adopt this value for the total nebular λ4686 flux. Dereddening this using E(B–V) = 0.069 gives I(4686) = 1.63×10^{-14} ergs cm^{-2} s^{-1}.

The models of Schmutz et al. (1989, 1992) are parameterized by the transformed radius R_t and the stellar temperature T_*. In order to compare our derived ionization rates to these models, we need to transform R_t into the stellar radius R_*, via equation 1 of Schmutz et al. (1992) which gives R_t as a function of R_*, v_∞ and $\dot{M}$. The terminal wind velocity, v_∞, was derived for DR 1 in the previous section, however $\dot{M}$ for DR 1 cannot be derived straightforwardly. The only WO star with a known mass loss rate is Sand 5, a WO2 star in the galactic open cluster Be 87, whose $\dot{M}$ = 1.7×10^{-5} M$_\odot$ yr^{-1} (Barlow 1991). In order to obtain $\dot{M}$ for DR 1, we have scaled the $\dot{M}$ derived for Sand 5 in the following manner. When the opacity is dominated by electron scattering (or by bound-free or free-free opacity and the flows have similar electron temperatures), the luminosity in a stellar He II emission line scales with the mass loss rate in the same way as the radio free-free flux, i.e. $L_L \propto (\gamma^{1/2}\dot{M}/v_\infty)^{4/3}$ (cf. Morris et al. 1993b), where γ is the number of free electrons per He^{2+} ion, equal to 5.93 for DR 1 and 4.67 for Sand 5. The luminosity L_L in a stellar emission line such as He II 4686 Å is equal to $4\pi D^2 I_L$, where D is the distance to the star and I_L is the dereddened flux in the stellar He II 4686 Å line, listed in Table 4 for DR 1 and in Table 5 of KBS for Sand 5. Thus the mass loss rate $\dot{M}$ for DR 1 may be expressed as:

© European Southern Observatory • Provided by the NASA Astrophysics Data System

1995A&A...295..171K

Table 6. Logarithmic continuum fluxes for DR 1, in cgs units

λ^*(Å)	4200	4400	4800
$F_\lambda(TOT)$	−16.00	−16.11	−16.17
$F_\lambda(nebcont)$	−16.41	−16.44	−16.48
$F_{star}(\lambda^*)$	−16.21	−16.38	−16.45

$$\dot{M}\ (\mathrm{DR\ 1}) = \left(\frac{I_{4686}^{\mathrm{DR\ 1}}}{I_{4686}^{\mathrm{Sand\ 5}}}\right)^{3/4} \left(\frac{D(\mathrm{DR\ 1})}{D(\mathrm{Sand\ 5})}\right)^{3/2} \frac{v_\infty(\mathrm{DR\ 1})}{v_\infty(\mathrm{Sand\ 5})} \times \left(\frac{\gamma(\mathrm{Sand\ 5})}{\gamma(\mathrm{DR\ 1})}\right)^{1/2} \dot{M}\ (\mathrm{Sand\ 5}) \quad (4)$$

and is equal to 2.9×10^{-5} $M_\odot$ yr^{-1}. Equation 1 of Schmutz et al. (1992) thus yields $R_*=R_t/2.48$.

Table 6 presents the total continuum fluxes at λ^* measured in our wide-slit central 4.8 arcsec extraction, $F_\lambda(TOT)$; the theoretical nebular continuum fluxes, $F_\lambda(nebcont)$; and the resulting stellar continuum fluxes $F_{star}(\lambda^*)$. Table 7 presents the derived Zanstra ratios R(H I) and R(He II), and the derived total ionizing photon rates N(H I) and N(He II) for DR 1. Table 7 also presents various model predictions for R(H I), R(He II), N(H I) and N(He II), along with the following parameters for the Schmutz et al. (1989) (β = 1) and 1992 (β = 2) models: the velocity law β, the stellar temperature T_*, the 'transformed' radius R_t, and the stellar radius R_*.

For the models, the ionizing photon rate $N_{ion} = 4\pi R_*^2\ n_{ion}$, where n(H I) and n(He II) are denoted as Q_0 and Q_2 respectively by Schmutz et al. (1989, 1992). Our derived I(4686)/I(Hβ) ratio of 0.048 implies an N(He II)/N(H I) ratio of 0.026, in agreement with the value estimated by Garnett et al. (1991). The nebula is almost certainly optically thick in the He II ionizing continuum but could be optically thin in the H I Lyman continuum, so that the derived values of R(H I) and N(H I) could be underestimates.

Amongst the β = 1 models of Schmutz et al. (1989) listed in Table 7, the T_* = 75000 K, R_t = 14 and 16 $R_\odot$ models both provide a good match to the observed value of R(H I), with the R_t = 16 $R_\odot$ model providing the better match to R(He II) and the R_t = 14 $R_\odot$ model providing the better match to N(He II). However, the luminosities of both models are very similar (final column of Table 7). The 90000 K β = 1 models listed in Table 7 do not provide a good fit to the observations. Amongst the β = 2 models of Schmutz et al. (1992), the T_* = 74100 K R_t = 9.52 $R_\odot$ model (not listed in Table 7) has an R(He II) value which is 0.7 dex smaller than the observed value. Amongst the two β = 2 models listed in Table 7, the T_* = 93500 K, R_t = 9.52 $R_\odot$ model overestimates R(He II) by 0.9 dex, while the T_* = 95600 K, R_t = 4.37 $R_\odot$ model, although able to match N(He II), underestimates N(H I) by 0.4 dex.

The 75000 K β = 1 models, which provide the closest match to the observations, imply that $\log(L/L_\odot) = 6.0\pm0.2$ for DR 1. These values can be compared to the luminosity that Esteban et al. (1993) derived for Sand 4, a galactic WO1 star, by using a Schmutz et al. (1992) β = 2 extended model atmosphere to carry out photoionization modelling of G2.4+1.4, the nebula around Sand 4. They obtained T_* = 105000 K, R_* = 1.1 $R_\odot$, and $\log(L/L_\odot) = 5.08$ (for an adopted distance of 3 kpc, which is somewhat more uncertain than the distance to IC 1613; Dopita et al. (1990) derived a higher luminosity for Sand 4, but this was based on a blackbody model, so their results are not directly comparable). For the other WN and WC stars in their sample, Esteban et al. (1993) derived $\log(L/L_\odot)$ values ranging from 5.1 to 5.7. The two WO stars for which temperatures have now been derived are the hottest WR stars known. We find that the luminosity of the WO3 star DR 1, in the metal-poor dwarf galaxy IC 1613, is significantly higher than that of the WO1 star Sand 4, located in our own galaxy, consistent with evolutionary predictions (e.g. Meynet et al. 1994) that stars of lower initial metallicity will be more massive, and therefore more luminous, at the WR stages, due to less mass loss stripping during the earlier O and B supergiant stages.

4.2. WO star abundances

4.2.1. Method

In KBS, we derived stellar wind abundances via recombination theory for a sample of four WO stars. This method was originally used by Hummer et al. (1982) to derive the abundances for the WC8 star γ Vel, and has been used since to derive relative abundances for a large number of WR stars (e.g. Torres 1988; Smith & Hummer 1988; Eenens & Williams 1992, KBS). Recombination theory presents the most straightforward way of deriving abundances in the winds of WR stars, and the final abundances have been found to be in agreement with those derived via complete non-LTE model atmosphere modelling of the winds (e.g. Hillier 1989; Hamann et al. 1992), which have only been completed for a handful of stars. The full details of the method employed here are described in Sect. 8.2 of KBS, along with a full discussion of the limitations in deriving abundances using this method.

Here, we only briefly outline our case B recombination analysis. The dereddened line intensity I of a recombination line at wavelength λ can be related to the number density of the emitting ionic species $n(X^{p+})$ integrated over the volume of emission via

$$[n(X^{+p})] \propto I(\lambda)/Q(\lambda) \quad (5)$$

where Q is defined as $h\nu\alpha_{\mathrm{eff}}^{rec}$ and h is Planck's constant, ν is the frequency of the line and $\alpha_{\mathrm{eff}}^{rec}$ is the effective recombination coefficient, which can include dielectronic as well as radiative recombination contributions. Thus one may straightforwardly obtain the relative abundance of two species $n(X)$ and $n(Y)$ by adding all stages of ionization present:

$$\frac{n(X)}{n(Y)} = \frac{\sum_p [n(X^{p+})]}{\sum_q [n(Y^{q+})]} \quad (6)$$

For the present analysis (as in KBS), we have adopted T_e = 50000 K and $n_e = 10^{11}$ cm^{-3} as representative for the stellar

© European Southern Observatory • Provided by the NASA Astrophysics Data System

1995A&A...295..171K

Table 7. Logarithmic H I and He II Zanstra ratios, R(H I) and R(He II), in cgs units; logarithmic total ionizing photon rates, N(H I) and N(He II), in cgs units; and logarithmic stellar luminosities, in solar units.

Model Parameters				λ4200		λ4400		λ4800				
β	T_* (K)	$R_t/R_\odot$	$R_*/R_\odot$	R(H I)	R(He II)	R(H I)	R(He II)	R(H I)	R(He II)	N(H I)	N(He II)	$L/L_\odot$
1	75000	14.0	5.65	16.03	14.20	–	–	16.25	14.41	49.84	48.00	5.96
1	75000	16.0	6.45	16.04	14.45	–	–	16.25	14.65	49.94	48.34	6.08
1	90000	5.0	2.00	15.95	14.78	–	–	16.12	14.95	49.12	47.95	5.37
1	90000	13.0	5.24	16.16	15.17	–	–	16.36	15.37	49.97	48.98	6.21
2	93500	9.52	3.81	–	–	16.16	15.30	–	–	49.79	48.93	6.00
2	95600	4.37	1.75	–	–	15.99	14.83	–	–	49.18	48.02	5.36
DR 1				16.08	14.50	16.25	14.67	16.31	14.78	49.59	48.01	

The β=1 models are from Schmutz et al. (1989), and the β=2 models are from Schmutz et al. (1992). R_t is the 'transformed' radius given by equation 1 of Schmutz et al. (1992). For DR 1, $R_* = R_t/2.48$ – see text.

wind electron temperature and density. References for the recombination coefficients are given in Sect. 8.2 of KBS, and the values of Q are listed in Table 11 of KBS. Table 8 presents the I/Qs derived for each transition, as well as the final I/Q which we have adopted for each ionic species. This is a weighted average, and the weighting is based on the S/N of the line in particular, and whether it was a substantial fractional contributor to the given feature or not. Individual cases are described below. Lines which we suspect to be optically thick, or partially thick, were given zero weight in the final average.

4.2.2. Final abundances

The final abundances by number were derived by summing all stages of ionization present. In the case of helium, He^{2+} is the only stage of ionization seen and in the case of carbon, C^{4+} is the only stage of ionization present, so the C^{4+}/He^{2+} ratio provides a good estimate of the C/He ratio. In the case of oxygen, O^{4+}, O^{5+} and O^{6+} are all seen, hence the O/He ratio is the sum of the O^{m+}/He^{2+} ratios. For KBS, oxygen abundances were more straightforward to derive, as their spectral coverage extended from the UV to the near-IR, and lines from all stages of ionization were seen. Here, we only have lines from the optical region to utilize, and the O IV and O V lines in this region are partially optically thick and their line strengths cannot be straightforwardly interpreted using recombination theory, as discussed in Sect. 8.3.1 of KBS. Our method to derive the oxygen abundance for DR 1 is described below. In KBS, higher stages of ionization of oxygen (O^{7+}, O^{8+}) and carbon (C^{5+}) were only weakly seen in the spectra of the WO1 star, Sand 4, and were not seen at all in the spectra of the WO2 star Sand 5, hence for DR 1, a WO3 star, a significant contribution from higher stages of ionization would not be expected.

He^{2+}: The I/Q for He^{2+} was derived from a weighted average of the 4–3 and 7–4 transitions at 4686 Å and 5411 Å respectively. Although the 4–3 transition is not the major contributor to the blend of He II+C IV at 4658+86 Å, it is the strongest He II feature present and hence is highly weighted. Additionally, the S/N of the 5411 Å feature is poor. The 6–4 transition at 6562 Å is blended with nebular Hα, hence its flux is very uncertain, and was not incorporated in either the He^{2+} or C^{4+} final I/Q.

Table 8. I/Qs for DR 1

ion	trans	I/Q	weight
He^{2+}	4686 (4–3)	2.42×10^{10}	3
	5411 (7–4)	2.09×10^{10}	1
	6561 (6–4)	5.0×10^{10}	0
Adopted		2.33×10^{10}	
C^{4+}	3690 (9–6,15–7,14–7)	(1.52×10^{10})	0
	4658,86 (6–5,8–6)	1.57×10^{10}	2
	5411 (14–8)	(1.38×10^{10})	0
	5470 (10–7)	8.4×10^{9}:	0
	5801,12 (3p $^2P^0$–3s ^2S)	1.22×10^{10}	0
	6560 (12–8)	(1.5×10^{10})	0
	7062 (9–7)	1.53×10^{10}	1
	7726,36 (70–6,11–8,14–9)	1.40×10^{10}	1
Adopted		1.52×10^{10}	
O^{4+}	3400 (3d ^2D–3p $^2P^0$)	5.22×10^{9}	0
Adopted		**	
O^{5+}	5590 (3d ^3D–3p $^3P^0$)	6.88×10^{8}	0
Adopted		**	
O^{6+}	3434,36 (7–6,11–8)	(1.48×10^{9})	0
	3811,34 (3p $^2P^0$–3s ^2S)	1.24×10^{10}	0
	5290 (8–7)	1.48×10^{9}	1
Adopted		1.48×10^{9}	

Notes to Table 8: ** See text for a discussion of the adopted I/Qs for O^{4+} and O^{5+}.

C^{4+}: The C^{4+} I/Q was derived from the transitions at 4658+86 Å(6–5,8–6), 7062 Å (9–7) and 7726 Å (7–6,11–8,14–9). C IV is a major contributor to the 4658+86 Å blend with He II, and the other lines included in the weighted average are purely due to C IV. The 7726 Å feature suffers from telluric absorption by the atmospheric A-band on the shortward side for

© European Southern Observatory • Provided by the NASA Astrophysics Data System

1995A&A...295..171K

the WO1 and WO2 stars, however, this is not the case for DR 1, a WO3 star, as it has a much lower wind expansion velocity in comparison. Additionally, the I/Q from 7726 Å is in reasonable agreement with that from 7062 Å. Other C IV features were not included in the final I/Q average as they were either weak, or minor contributors to blends. The 3p $^2P^0$ – 3s ^2S transition at 5801,12 Å was found to have an I/Q a factor of 1.25 smaller than the I/Qs derived from the other C IV lines. Similarly, the I/Q derived from this line for Sand 1, the WO4 star in the SMC, was a factor of 1.3 smaller than derived from the other C IV lines, and was factors of 2–6 smaller for the WO1 and WO2 stars. The complete mechanism for producing this line is not yet understood and the observed line strength is unable to be duplicated in detailed atmospheric models for WC stars (e.g. Hillier 1989).

O^{6+}: The I/Q for O^{6+} was derived from the 8–7 transition at 5290 Å. The I/Q given by the 3p $^2P^0$–3s ^2S transition at 3811,34 Å is a factor of 8.4 higher than the adopted I/Q. The strength of this transition (which defines the WO class of stars) is also enhanced, by factors of 4–12, in the other WO stars.

O^{4+}, O^{5+}: The 3d ^3D–3p $^3P^0$ transition of O V at 5590 Å and the 3d ^2D–3p $^2P^0$ transition of O IV at 3400 Å both arise from low-lying transitions and so are potentially optically thick, and were found by KBS to give lower and higher I/Qs respectively, than the higher-lying O^{4+} and O^{5+} lines in the case of the WO4 stars. In order to estimate the O^{4+} and O^{5+} abundances, we used the fact that for DR 1 the EW(O V 5590)/EW(O VI 5290) ratio is 0.87 times the ratio measured by KBS for Sand 1 (the WO4 star in the SMC), so since the ratio O^{5+}/O^{6+} is 2.44 for Sand 1, we adopt a value of 2.11 for this ratio for DR 1. Similarly, the EW(O IV 3400)/EW(O VI 5290) ratio for DR 1 is 0.49 of the ratio measured by KBS for Sand 1, so since O^{4+}/O^{6+} for Sand 1 is 2.44, we adopt a value of 1.20 for this ratio for DR 1. Clearly it would be desirable to obtain UV spectra of this object, in order to carry out a more accurate analysis of the O^{4+} and O^{5+} abundances.

The final abundances for DR 1, by number and by mass respectively, are presented in Tables 9 and 10.

Table 9. Abundances for DR 1

By no.	C^{4+}/He^{2+}	0.65
	O^{4+}/He^{2+}	(0.076)
	O^{5+}/He^{2+}	(0.13)
	O^{6+}/He^{2+}	0.063
	C/He	0.65
	O/He	0.27
	C/O	2.4
	(C+O)/He	0.92

Table 10. Abundances by mass for DR 1, Sand 1 and the Meynet et al. (1994) evolutionary models

	X_{He}	X_C	X_O	initial Z
DR 1 (WO3) logL=6.0, logT=4.88	0.25	0.48	0.27	0.001
Sand 1 (WO4)	0.22	0.52	0.26	0.003
120 $M_\odot$, stage 37, τ=3.1×10^6 yr, present M=26 $M_\odot$ logL=5.96, logT=4.39	0.21	0.33	0.46	0.001
60 $M_\odot$, stage 38, τ=4.1×10^6 yr, present M=10.6 $M_\odot$ logL=5.33, logT=4.59	0.26	0.44	0.29	0.004
85 $M_\odot$, stage 38, τ=3.5×10^6 yr, present M=11.5 $M_\odot$ logL=5.40, logT=4.58	0.25	0.42	0.32	0.004
120 $M_\odot$, stage 38, τ=3.2×10^6 yr, present M=9.8 $M_\odot$ logL=5.28, logT=4.60	0.27	0.44	0.28	0.004

4.2.3. Discussion

The abundances derived for DR 1 are similar to those found for the other WO stars by KBS (see Tables 15 and 16 of KBS). In the present study, the C/He ratio for DR 1 is more accurately known than is the O/He ratio, however the O/He ratio derived here is also similar to that found for Sand 1, the WO4 star in the SMC (Table 10). If we simply multiplied the derived O^{6+}/He^{2+} abundance ratio for DR 1 by the O/O^{6+} abundances of Sand 1 and Sand 2 (the two WO4 stars), we would obtain O/He number ratios of 0.24 and 0.20 respectively, compared to the value of 0.27 in Table 9. It is likely that the overall O/He abundance ratio would vary by much less than a factor of two if the abundances in the O^{4+} and O^{5+} stages could be more accurately estimated.

The carbon abundance for DR 1 derived here is at the top end of the range found for the early WC type stars by Torres (1988), Smith & Hummer (1988) and Eenens & Williams (1992), but its carbon mass fraction of 0.48 is only slightly lower than the values of 0.51–0.53 derived by KBS for four other WO stars. A slightly lower mass fraction for carbon is predicted throughout the helium-burning stages in the most recent evolutionary models of Meynet et al. (1994), who have included mass loss rates which are enhanced by a factor of two over the 'standard' mass loss rates of Schaller et al. (1992) during the main sequence and WNL stages (i.e. when the stellar winds are believed to be essentially driven by radiation pressure). In a comparison of the WC abundances derived by Smith & Hummer (1988) with the models of Schaller et al. (1992), Schaerer & Maeder

© European Southern Observatory • Provided by the NASA Astrophysics Data System

1995A&A...295..171K

(1992) noted that increased mass loss rates were required to bring the model predictions in line with what was derived observationally. In KBS, we found that, when comparing them to the abundances derived for both the Galactic and Magellanic Cloud WO stars, the enhanced mass loss rate models of Meynet et al. (1994) were better able to reproduce the observed oxygen mass fractions than the models of Schaller et al. (1992)

Meynet et al. also predicted that for the WO model stages at LMC metallicity (Z = 0.008), the He, C and O abundances should not differ significantly from those for galactic metallicity models, in agreement with the similar abundances derived by KBS for Sand 2, an LMC WO4 star, and the two galactic WO1 and WO2 stars, Sand 4 and Sand 5. KBS also found that the higher oxygen and lower helium abundances predicted for the WO stage by the Z = 0.004 models of Meynet et al., compared to the higher metallicity models, were in better agreement with the results they obtained for Sand 1, the WO4 star in the SMC (initial Z = 0.003).

A comparison of the abundances by mass that we have derived for DR 1 with the Z = 0.001 models of both Schaller et al. (1992) and the enhanced mass loss rate models of Meynet et al. (1994) reveals generally poor agreement. In the lowest metallicity (Z = 0.001) models of Schaller et al., the WC/WO stages are never reached (because of the lower metal opacity, radiation pressure does not strip away the hydrogen-containing envelope during the earlier evolutionary stages). However, with the enhanced mass loss rates adopted by Meynet et al., the products of helium burning are revealed in their 85 $M_\odot$ and 120 $M_\odot$ models. But in these two models the conversion of He and C into O appears to be too fast, i.e. the models predict too high oxygen abundances and too high (C+O)/He ratios compared to those we see. The nearest agreement is found with the Z = 0.001 120$M_\odot$ model at stage 37 (Table 10), the first stage without surface hydrogen. The model surface mass fractions are: X(He) = 0.21, X(C) = 0.33 and X(O) = 0.46; while the observed mass fractions for DR 1 are X(He) = 0.25, X(C) = 0.48, X(O) = 0.27. Even if our O/He relative abundance was to be increased by a factor of two, the evolutionary model would still somewhat underestimate X(C). On the other hand, the abundances derived for DR 1 are quite similar to those found for Sand 1 (in the SMC, where Z = 0.003), and good agreement is found with stage 38 of the 60 $M_\odot$, 85 $M_\odot$ and 120 $M_\odot$ Z = 0.004 enhanced mass loss rate models of Meynet et al. (1994), although the predicted mass fractions of carbon are still somewhat low, and the predicted mass fractions of helium somewhat high. Table 10 presents the relevant mass fractions. The abundances we have derived for DR 1 indicate that the factor of three difference in the metallicities of IC 1613 and the SMC has had little effect on the surface abundances of stars in the WO stage in these galaxies.

The luminosity listed in Table 10 for stage 37 of the Z = 0.001 120 $M_\odot$ model of Meynet et al. (1994) is consistent with the luminosity of 10^6 $L_\odot$ that we derived in Sect. 4.1. The Z = 0.004 models of Meynet et al., while better able the observed stellar surface abundances, predict too low a luminosity for DR 1. The stellar temperatures predicted by Meynet et al. (see Table 10) are defined in a different manner from those of Schmutz et al. used here and so cannot be directly compared with our results.

Although the results presented here and by KBS for the WO stars show relatively good agreement as a function of metallicity with the abundances by Meynet et al. (1994), it is important to keep in mind the other parameters which affect the surface abundances of WR stars, to test if varying these also can produce the abundances which we have derived empirically. For example, the surface abundances are also sensitive to overshooting and the extension of the convective core (Meynet et al. 1994); overshooting enlarges the core and thus less mass in the envelope needs to be peeled off to reveal the core, and accordingly lower C and O abundances (compared to the 'standard' mass loss rate models of Schaller et al.) are obtained at the beginning of the WC phase. In addition, the rate for the $^{12}C(\alpha,\gamma)^{16}O$ reaction is still disputed and could significantly affect the abundances predicted after entry into the WC stage. Hence it would be desirable to compute models varying these other parameters, to test the uniqueness of the present models' predictions for the surface abundances of WR stars.

Acknowledgements. We would like to thank the staff at the La Palma Observatory for obtaining these observations during service time, Werner Schmutz for kindly providing files containing his NLTE extended WR models and Donald Garnett for helpful comments on the paper.

References

Armandroff, T.E., Massey, P. 1985, ApJ 291, 685
Armandroff, T.E., Massey, P. 1991, AJ 102, 927
Barlow, M.J., 1991, in IAU Symp. No. 143, Wolf-Rayet Stars and Interrelations with other Massive Stars in Galaxies, ed. K.A. van der Hucht and B. Hidayat, Kluwer, Dordrecht, 281
Barlow, M.J., Hummer, D.G. 1982, in Proc. IAU Symp. No. 99, Wolf–Rayet Stars: Observations, Physics, Evolution, ed. C.W.H. de Loore & A.J. Willis, Reidel, Holland, 79
Burstein, D., Heiles, C. 1982, AJ 87, 1165
Chu, Y.-H. 1991, in: IAU Symp. No. 143, Wolf-Rayet Stars and Interrelations with other Massive Stars in Galaxies, eds. K.A. van der Hucht & B. Hidayat, Dordrecht, 349
Clegg, R.E.S. 1987, MNRAS 221,31p
Clegg, R.E.S., Middlemass, D. 1987, MNRAS 228, 759
Davidson, K., Kinman, T.D. 1982, PASP 94, 634 (DK82)
Dopita, M.A., Lozinskaya, T.A., McGregor, P.J., Rawlings, S.J. 1990, ApJ 351, 563
Dopita, M.A., Binette, L., D'Odorico, S. & Benvenuti, P. 1984, ApJ 276, 653
D'Odorico, S., Rosa, M. 1982, A&A 105, 410
Dufour, R.J. 1984, in: IAU Symp. No. 108, eds. S. van der Bergh & K.S. de Boer, Dordrecht, Holland, p. 353
Eenens, P.R.J., Williams, P.M. 1992, MNRAS 255, 227
Esteban, C., Smith, L.J., Vílchez, J.M., Clegg, R.E.S. 1992, A&A 259, 629
Esteban, C., Smith, L.J., Vílchez, J.M., Clegg, R.E.S. 1993, A&A 272, 299
Fitzpatrick, E.L. 1985, ApJS 59, 77
Garnett, D.R., 1990, ApJ 363, 142

© European Southern Observatory • Provided by the NASA Astrophysics Data System

1995A&A...295..171K

Garnett, D.R., Kennicutt, R.C., Chu, Y., Skillman, E.D. 1991, ApJ 373, 458
Garnett, D.R., Chu, Y.-H., Dopita, M.A. 1993, RevMexA&A 27, 141
Hamann, W.-R., Leuenhagen, U., Koesterke, L. 1992, A&A 255, 200
Henry, R.B.C. 1990, ApJ 356, 229
Hillier, D.J. 1989, ApJ 347, 392
Hodge, P.W. 1978, ApJS 37, 145
Hodge P.W., Lee, M.G., Gurwell, M. 1990, PASP 102, 1245
Howarth, I.D., Murray, J. 1990 SERC STARLINK User Note No. 50
Hummer, D.G., Storey, P.J. 1987, MNRAS 224, 801
Hummer, D.G., Barlow, M.J., Storey, P.J. 1982, in: IAU Symp. No. 99, Wolf–Rayet Stars: Observations, Physics, Evolution, ed. C.W.H. de Loore & A.J. Willis, Reidel, Holland, p. 79
Hunter, D.A., Gallagher, J.S. 1985, ApJS 58, 533
Husfield, D., Kudritzki, R.P., Simon, K.P., Clegg, R.E.S. 1984, A&A 134, 139
Kingsburgh, R.L., Barlow, M.J. 1994, MNRAS, 271, 257
Kingsburgh, R.L., Barlow, M.J., Storey P.J. 1994, A&A, in press (KBS)
Kwitter, K.B. 1984, ApJ 287, 840
Lake, G., Skillman, E.D. 1988, AJ 98, 1274
Maeder, A. 1990, A&AS 94, 139
Meynet, G., Maeder, A., Schaller, G., Schaerer, D., Charbonnel, C. 1994, A&AS 103,97
Morris, P.W., Brownsberger, K.R., Conti, P.S., Massey, P., Vacca, W.D. 1993a, ApJ 412, 434
Morris, P.W., Conti, P.S., Lamers, H.J.G.L.M. & Koenigsberger 1993b, ApJ 414, L25
Oke, J.B., 1990, AJ 99, 1621
Pakull, M.W. 1991, in IAU Symp. No. 143, Wolf-Rayet Stars and Interrelations with other Massive Stars in Galaxies, ed. K.A. van der Hucht and B. Hidayat, Kluwer, Dordrecht, 391
Peimbert, M., Bohigas, J.B., Torres-Peimbert, S. 1988, RevMexA&A 16, 45
Price J.S., Mason, S.F., Gullixson, C.A. 1990, AJ 100, 420
Saha, A., Freedman, W.L., Hoessel, J.G., Mossman, A.E. 1992, AJ 104, 1072
Seaton, M.J. 1979, MNRAS 187, 73p
Sandage, A.R. 1971, ApJ 166, 13
Schaller, G., Schaerer, D., Meynet, G., Maeder, A. 1992, A&AS 96, 269
Schaerer, D., Maeder, A. 1992, A&A 263, 129
Schild, H., Testor, G. 1991, A&A 243, 115
Schild, H., Smith, L.J., Willis, A.J. 1990, A&A 237, 169
Schmutz, W., Hamann, W.R., Wessolowski, U. 1989, A&A 210, 236
Schmutz, W., Leitherer, C., Gruenwald, R. 1992, PASP 104, 1164
Skillman, E.D., Kennicutt, R.C. & Hodge, P.W., 1989, ApJ 347, 875
Smith, L.F., Hummer, D.G. 1988, MNRAS 230, 511
Smith, L.F., Maeder, A. 1990, A&A, 241, 77
Stasinska, G. 1980, A&A 84, 299
Stasinska, G. 1982, A&A 48, 299
Talent, D.L. 1980, Ph.D. Thesis, Rice University
Torres, A.V. 1988, ApJ 325, 759
Walton, N.A., Barlow, M.J., Clegg, R.E.S. & Monk, D.J., 1994, in preparation
Willis, A.J., Schild, H., Smith, L.J. 1992, A&A 261, 419

This article was processed by the author using Springer-Verlag LaTeX A&A style file version 3.

© European Southern Observatory • Provided by the NASA Astrophysics Data System